Asian Journal of Chemistry; Vol. 33, No. 2 (2021), 281-290

ASIAN JOURNAL OF CHEMISTRY

https://doi.org/10.14233/ajchem.2021.22953

Calcium Alginate Beads Doped with Nano-ZrO_2 and Activated Carbon of *Annona reticulate* Plant as an Effective Adsorbent for Water Remediation of Chromium(VI)

WONDWOSEN KEBEDE BIFTU[1,2] and KUNTA RAVINDHRANATH[1,*]

[1]Department of Chemistry, Koneru Lakshmaiah Education Foundation, Green Fields, Vaddeswaram-522502, India
[2]Ethiopian Radiation Protection Authority, Addis Ababa, Ethiopia

*Corresponding author: E-mail: ravindhranath.kunta@gmail.com

Received: 19 August 2020; *Accepted*: 30 September 2020; *Published online*: 15 January 2021; AJC-20210

An activated carbon produced from stems of *Annona reticulate* plant (SACAR) by conc. H_2SO_4 digestion, is observed to have strong affinity for toxic Cr(VI) ions. Its adsorptivity for Cr(VI) ions was enhanced by admixing it with 'nano-ZrO_2' (Zr-SACAR)-synthesized adopting green methods. For ensuring easy filtration, the 'active carbon + nanoparticle composite' was immobilized in calcium alginate beads (Zr-SACAR-Ca). Optimum extraction conditions for these three adsorbents for the removal of Cr(VI) ions from water were investigated. The adsorption capacities were found to be 92.2 mg/g for SACAR; 109.83 mg/g for Zr-SACAR and 119.34 mg/g for Zr-SACAR-Ca. The sorption nature was characterized by XRD, FTIR, FESEM and EDX studies. The sorption mechanism was investigated using various isotherm models. Thermodynamic studies revealed the endothermic and spontaneous nature of sorption. The kinetics of adsorption was well defined by the pseudo-second-order model. The spent adsorbent are regenerated and reused until six cycles with marginal decrease in Cr-adsorptivity. The adsorbents developed are effectively applied in the treatment of polluted water samples collected from Ethiopia.

Keywords: Nano zirconium oxide, Green method, Active carbon, *Annona reticulate*, Cr(VI) water remediation.

INTRODUCTION

The toxicity of chromium ions is well known and out of the tri- and hexavalent states of chromium, the latter is more toxic [1]. Chromium species enter into the water bodies mainly due to the ill-treated effluents disposal from various chromium related industries. The maximum permissible level of total Cr is 50 ppb for drinking water as per WHO [2].

Various methods based on chemical reduction cum-precipitation [3-5], flocculation [4], electroplating-electrolysis [6,7], ion exchange [8], adsorption [9,10] and nano-filtration [11] are reported for the removal of chromium(VI). Of these, adsorption methods based on biomaterials are proving to be effective because the procedures are simple, effective and eco-friendly [12-14]. The merits of these active carbons are that they possess good sorption capacities, easy availability and based on renewable sources besides being economical and eco-friendly [15-18]. The recent trend is to employ nanomaterials as adsorbents for the water remediation in view of their high adsorptivities [19-21].

The composite adsorbents prepared from nanoparticles and active carbons have cumulative advantages of both the materials and they are proving to be more effective than individual substances [22-24]. But the main disadvantage of such composites as adsorbents in water purification is the problem involved in the filtration due the small size of the particles. This disadvantage can be overcome by immobilizing the composites in natural/synthetic polymers (organic/inorganic) preferably in beads.

The beads embedded with nanoparticles ensures the easy filtration and at the same time, the cumulative sorption nature of nanoparticles and active carbons, can be evoked for the successful removal of pollutants. Thus nanoparticle and active carbons are complementary for each other in enhancing the adsorptivity towards pollutants.

In the present investigation, an active carbon is derived from the stems of *Annona reticulate* (SACAR) by digesting it with conc. H_2SO_4. Nanoparticles of ZrO_2 of size 10-11 nm are successfully synthesized *via* green routes using hot water extract of skins of Sapindus plant seeds as 'capping and stabilizing

agent' and adopting the classical homogeneous methods of precipitation [25] from the viscous solution blend of water and ethylene glycol.

Active carbon (SACAR), composite comprising of active carbon and nano-ZrO_2 (Zr-SACAR) and calcium alginate beads embedded with the composite (Zr-SACAR-Ca), are studied as adsorbents for remediation of water for Cr(VI). These three adsorbents have been characterized using XRD, FTIR, FESEM and EDX techniques. The extractions conditions are investigated and optimized. The developed method is successfully applied to the effluent samples collected from the polluted rivers water in Ethiopia.

EXPERIMENTAL

A.R. grade chemicals were employed throughout the work. Simulated Cr(VI) stock solution of concentration: 500 mg/L was prepared and was diluted. A 0.25% of diphenyl carbazide in 50% of acetone and 6 N H_2SO_4, NaOH, $CaCl_2$, $ZrOCl_2{\cdot}8H_2O$, ethyl glycol, urea and Na-alginate were used.

Preparation of active carbon by treating conc. H_2SO_4: The precursor used for active carbon synthesis was the stems of *Annona reticulate* plant. The stem were cut to small pieces, washed with distilled water and sun-dried. Then the material was digested in conc. H_2SO_4 for overnight in a round bottomed flask with condenser set-up for 1 h. Biomaterial was completely carbonized. Thus generated carbon was filtered and washed repeatedly with double distilled water until the filtrate was neutral. Then the material was dried in an oven at 110 ºC for 6 h and sieved by 75 µm ASTM mesh. This active carbon was named as SACAR (sulphric acid activated carbon originated from stems of *Annona reticulata* plant).

Phytosynthesis of nano-ZrO_2: Nano-ZrO_2 of size 10.91 nm was synthesized using extraction of stems of Sapindus plant as capping agent and adopting homogeneous method of generating precipitating agent as described by Biftu and Ravidhranath [26]. In this method, the precipitant (OH^-) was slowly generated by urea-hydrolysis and thereby super saturation was minimized. This eliminates the undesirable local concentration effects in the solution, which are inevitably associated with the conventional precipitation process [25]. Further, by increasing in the viscosity of mother liquor using blends of water and ethylene glycol (for decreasing the speed of diffusion of ZrO_2 particles) and also by employing a newly identified biosurfactants capping agent, the particle size of nano ZrO_2 was successfully controlled [26].

Composite of active carbon and nZrO_2 (Zr-SACAR): SACAR (2.0 g) and nZrO_2 (0.5 g) were mixed in a 100 mL of distilled water and heated the solution at 90 ºC with constant stirring for 5 h. The solution was then cooled to room temperature and centrifuged. A grey coloured composite obtained was washed repeatedly with deionized water till the washings were neutral. Then the material was dried at 120 ºC for 4 h in hot-air oven. The composite was nano zirconium oxide loaded SACAR and named as Zr-SACAR.

Zr-SACAR embedded in calcium alginate beads (Zr-SACAR-Ca): Sodium alginate (2.5 g) in 100 mL of deionized water was heated at 70 ºC with constant stirring until a gel like matrix was obtained. Then Zr-SACAR (2.5 g) was added to the contents of the beaker with constant stirring. A homogeneous solution was resulted and it was cooled to room temperature. This solution was added in dropwise using a 50 mL Burette into a previously cooled (10 ºC) 2% calcium chloride solution. These beads were filtered, washed and dried at 70 ºC for 5 h, and named as Zr-SACAR-Ca (nZO_2 loaded onto sulphric acid activated carbon derived from stems of *Annona reticulate* immobilized by calcium alginate beads). The methodologies of the preparation of the adsorbents are summarized in Fig. 1.

Characterization of adsorbents: Three adsorbents developed in the present investigation were characterized by XRD, FTIR, FESEM and EDX for the samples before and after adsorption of Cr(VI). The crystallographic studies of the samples were made by X-ray diffraction (XRD) using CuKα source at 1.54 Å (PAN analytical X-ray diffractometer). The morphology of the samples were studied using a scanning electron microscope (SEM, JSM-6400F). The SEM images were noted from different areas of adsorbent at 10.0 kV at varying resolutions using the JSM-7600F model instrument.

FT-IR spectra of SACAR, Zr-SACAR and Zr-SACAR-Ca adsorbents before and after chromium(VI) adsorption were measured by a Nicolet 6700 FT-IR spectrometer. The IR spectra of the samples were recorded on a BRUKER ALFA FTIR spectrophotometer using KBr pellet technique over the range 4000–500 cm^{-1}.

Adsorption experiments: Batch experiments were conducted using the adsorbents: SACAR, Zr-SACAR and Zr-SACAR-Ca [4,5,27]. Requisite amounts of adsorbents were added to100 mL of 50 ppm of Cr(VI) simulated solution at different pHs 2-12. The pH of the initial solutions were adjusted using dil. HCl or dil. NaOH. Then the flasks were agitated in a rotator shaker at 300 rpm at various agitation times. All the experiments were performed at 30 ºC. After the completion of the required time intervals of equilibration, the conical flasks were removed from the orbital shaker and then the adsorbents were removed from the mother liquor by filtration or by centrifugation. The initial and final concentrations of chromium were analyzed by diphenyl carbazide spectrophotometer method at λ_{max}: 540 nm uses UV and visible spectrophotometer (Elico) as described earlier [1].

The % removal of Cr(VI) and adsorption capacity of the SACAR, Zr-SACAR and Zr-SACAR-Ca were calculated by the following equations:

$$\text{Removal } (\%) = \frac{(C_o - C_i)}{C_o} \times 100 \quad (1)$$

$$q_e = \frac{(C_o - C_e)}{m} \times V \quad (2)$$

where m = mass of adsorbent (g), V = volume of the solution (L), C_o and C_e are the initial and final concentrations (mg/L) of Cr(VI) ions. The adsorptive nature of SACAR, Zr-SACAR and Zr-SACAR-Ca were studied by changing pH, sorbent concentration, contact time, initial concentration of Cr(VI) and temperature.

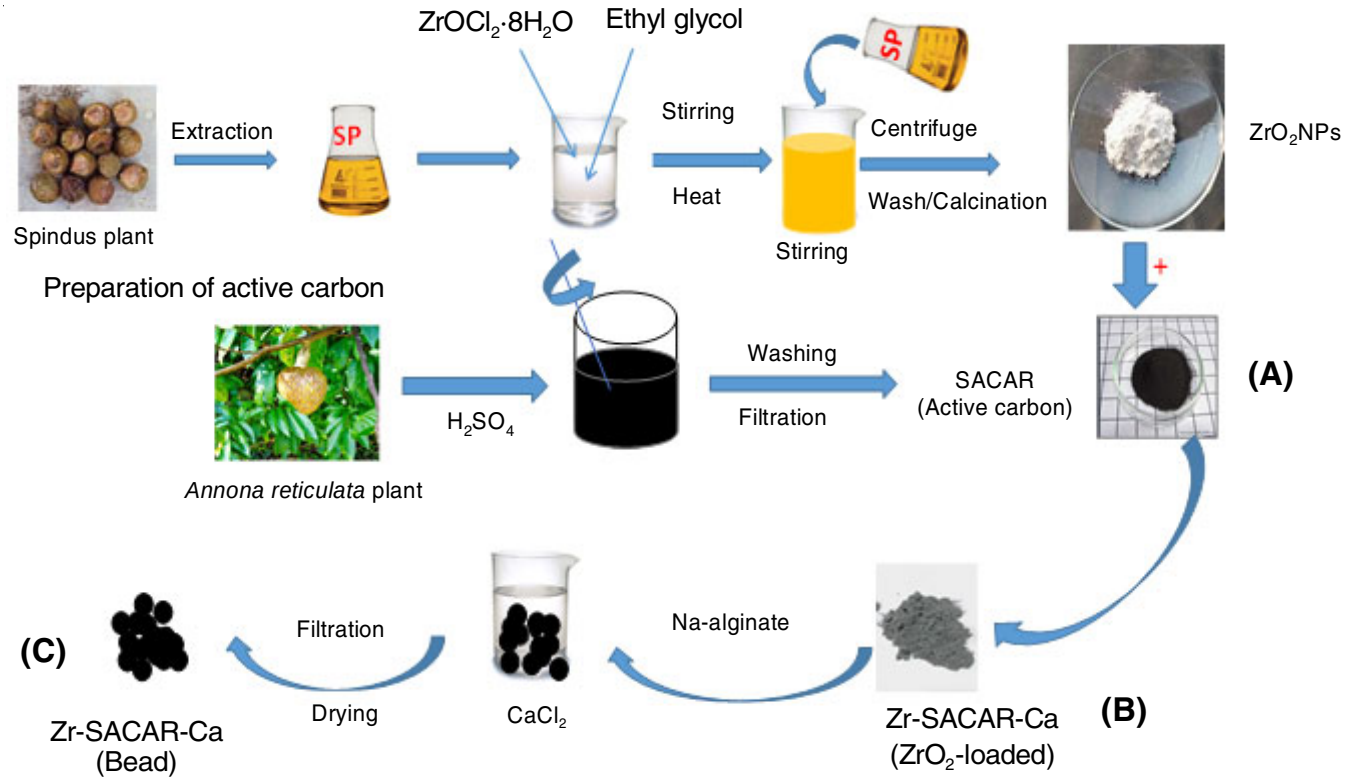

Fig. 1. Phases of preparation of SACAR, Zr-SACAR and Zr-SACAR-Ca

RESULTS AND DISCUSSION

FTIR analysis: The FTIR spectral features were observed for all the three adsorbents before and after adsorption of Cr(VI) and are presented in Fig. 2. It is interesting to note the changes in the band nature and positions of –OH frequencies before and after adsorption of Cr(VI) in all the three adsorbents. In case of the SACAR, broad peak ranging from 3490 to 3071 cm^{-1} with maxima at 3380.74 cm^{-1} pertaining to –OH groups is shifting towards higher wavenumber 3522-3083 cm^{-1} with maxima at 3387 cm^{-1}. Similarly, with Zr-SACAR as adsorbent, 3529-3185 cm^{-1} (b) with maxima at 3429.73 cm^{-1} shifted to 3490-3089 cm^{-1} (b) with maxima at 3384 cm^{-1}. In the case of Zr-SACAR-Ca, the broad band at 3505-3124 cm^{-1} with maxima at 3340.27 cm^{-1} shifted to 3539-3069 cm^{-1} (b) with small sharp peaks at 3401, 3340, 3127 cm^{-1}. The broadness reflects the hydrogen-bonding between the functional groups.

The changes in the peak positions and intensities indicate that there are interactions between Cr(VI) and functional groups of the three adsorbents. It is worth noting that in the case Zr-SACAR-Ca, sharp peaks (though less intensities) are appeared in addition to the broaden peak after adsorption of Cr(VI) and it may be due to a kind of order achieved on the surface of the adsorbent by strong interaction between Cr(VI) and surface function groups of Zr-SACAR-Ca; it may be a chemical in nature as is inferred from thermodynamic studies. Other frequencies were changed in position, intensities and nature of bands before and after adsorption of Cr(VI) in all the three adsorbents (Fig. 2). In case of SACAR, before adsorption, C-H and C=O frequencies are at 1706.63 and 2926.39 cm^{-1}, respectively and after adsorption, the C=O band was shifted to 1755.64 cm^{-1} and further, a doublet appeared at 2924 and 2856.18 cm^{-1}. This doublet was due to Fermi resonance pertaining to C-H in H-C=O. This indicates the presence of

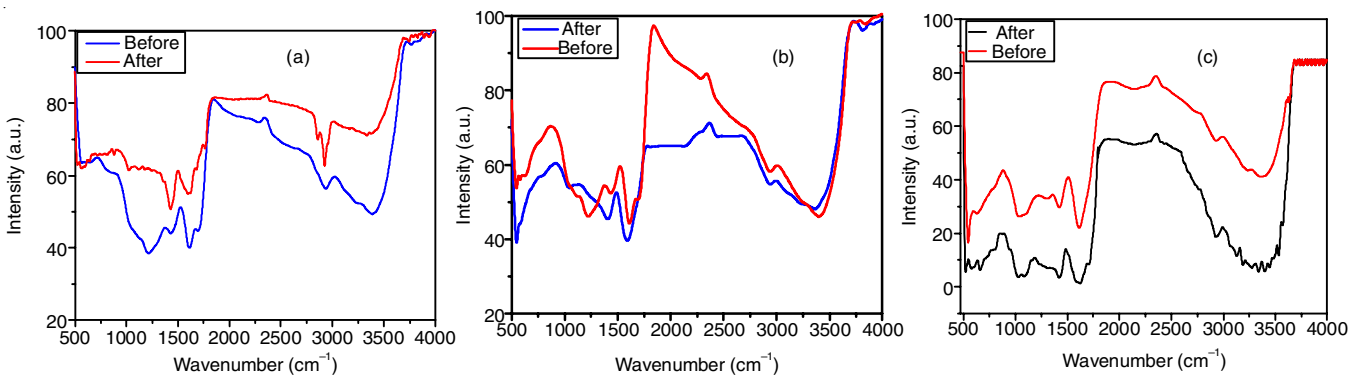

Fig. 2. FTIR spectra of SACAR (a); Zr-SACAR (b) and Zr-SAACAR-Ca (c) before and after Cr(VI) ion adsorption

aldehyde groups after adsorption in SACAR. Some sulfur related frequencies were also observed in all the adsorbents and expected because the active carbon was gene-rated *via* conc. H_2SO_4 treatment method. Thus, the FTIR study clearly indicated the major involvement of functional groups like –CO and –OH for the adsorption of Cr(VI) ion.

FESEM analysis: Surface morphologies of the SACAR, Zr-SACAR and Zr-SACAR-Ca were observed under FESEM (Fig. 3). On perusal of SEM images of all the three adsorbents, it was revealed that a dramatic contrast between the images taken before and after the adsorption of Cr(VI) ions The rough, micro pores, spongy, irregular and heterogeneous structures before adsorption had been changed to smoothly structures with the drastic decrease of pores, edges and corners. These features reflected that the adsorption of chromium(VI) had taken place and onto the surface of the adsorbents.

Energy dispersive X-ray spectroscopy (EDX): The EDX spectra of adsorbents (SACAR, Zr-SACAR and Zr-SACAR-Ca) before and after adsorption of Cr(VI) ions are shown in Fig. 4. A Cr-peak is present in after-adsorption spectra, which is absent before the adsorption process. This indicate that Cr(VI) was successfully adsorbed onto the surface of adsorbents (SACAR, Zr-SACAR and Zr- SACAR-Ca).

Effect of pH: The pHs of the solutions have profound influence on the sorption rate of adsorbates onto the surface of the adsorbents. The effect of pH on the adsorption of Cr(VI) was studied over the range from pH 2.0 to pH 12.0 while maintaining at optimum levels the other conditions of extraction namely: adsorbent concentration: 0.175 g/100 mL for SACAR, 0.15 g/100 mL for Zr-SACAR and 0.15 g/100 mL for Zr-SACAR-Ca; contact time: 40 min for SACAR, 45 min for Zr-SACRM and 45 min for Zr-SACRM-Ca; initial concentration of Cr(VI): 50 mg/L; rpm 300 and temperature 303 K. The obtained results were plotted as pH *vs.* % removal of Cr(VI) ions. It may be inferred from Fig. 5a that maximum Cr(VI) extractions were observed at pH: 2:90.08%for SACAR; 98.23% for Zr-SACAR' and 99.5% for Zr-SACAR-Ca.

These observations may be understood from the view point of pH_{zpc} of SACAR, Zr-SACAR and Zr-SACAR-Ca. The pH_{zpc} values evaluated from Fig. 6 were found to be 6.4, 6.6 and 6.7 for SACAR, Zr-SACAR and Zr-SACAR-Ca, respectively. At these pH_{zpc}, the surface of all the sorbents was neutral. Above these values, the surface acquires a negative charge due to dissociation of functional groups *viz.*, -OH, -COOH *etc.* and below positive charge due to protonation of the functional groups. So, at low pHs, the positive charge of the surface of the sorbents attracts negatively charged Cr(VI) species and hence, more adsorptivity. Above pH_{zpc}, the surface as well as Cr(VI) species were negatively charged and this results in repulsions and so, the adsorption decreases with increase in pH of solutions.

Effect of sorbent concentration: By varying the sorbent dosage from 0.05 to 0.3 g/100 mL, but maintain other extraction conditions at optimum levels, the adsorptivities of the sorbents for Cr(VI) were studied. The adsorption of Cr(VI) is progressively increased with the increase in dosage of adsorbent initially but it slows down with further increase in the dosage and attains a steady state at certain concentration of the adsorbent (Fig. 5b). The maximum extraction of Cr(VI) for the minimum dosage of adsorbent is found to be 92.58 %

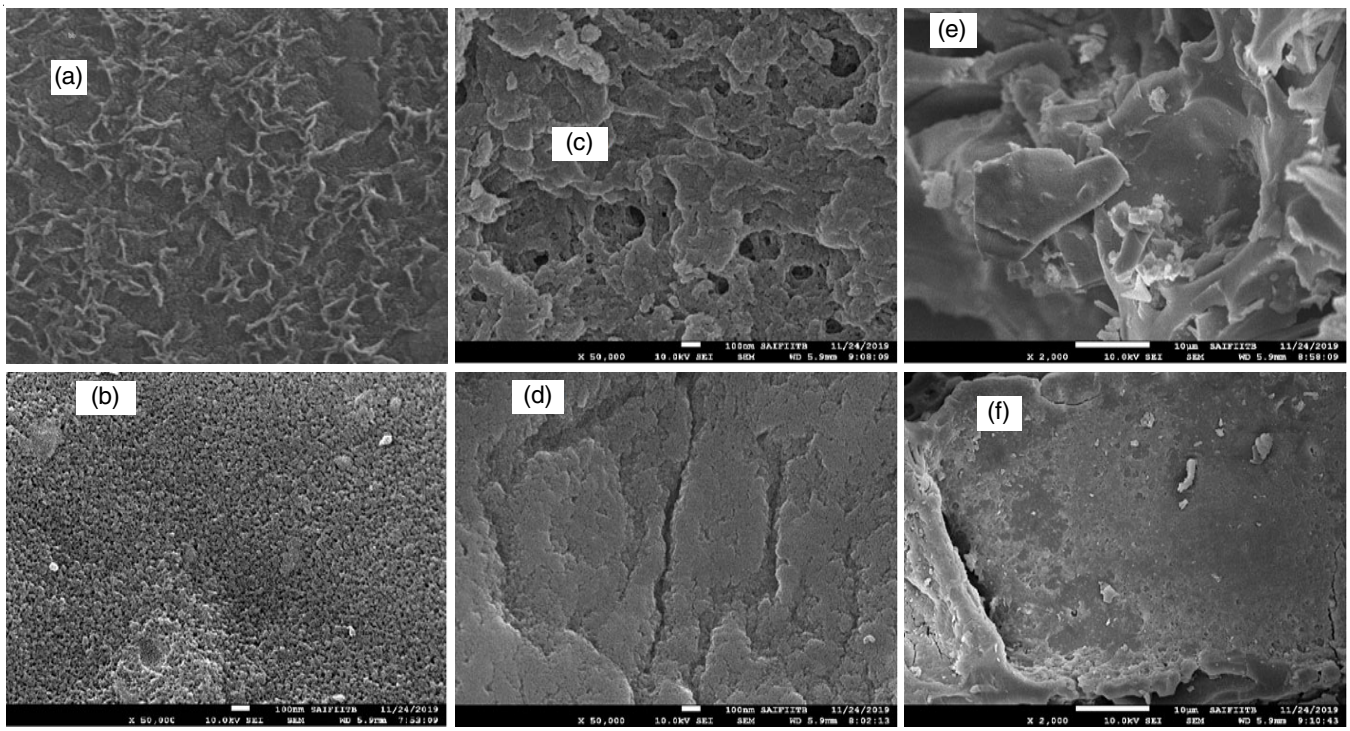

SEM images of active carbon: (a) SACAR (before), (b) SACAR (after)

SEM image of composite of active carbon and nano ZrO_2: (c) Zr-SACAR (before); (d) Zr-SACAR (after)

SEM image of beads: (e) Zr-SACAR-Ca alginate beads (before); (f)Zr- SACAR-Ca alginate beads (after)

Fig. 3. SEM image of SACAR, Zr-SACAR and Zr-SACAR-Ca alginate beads

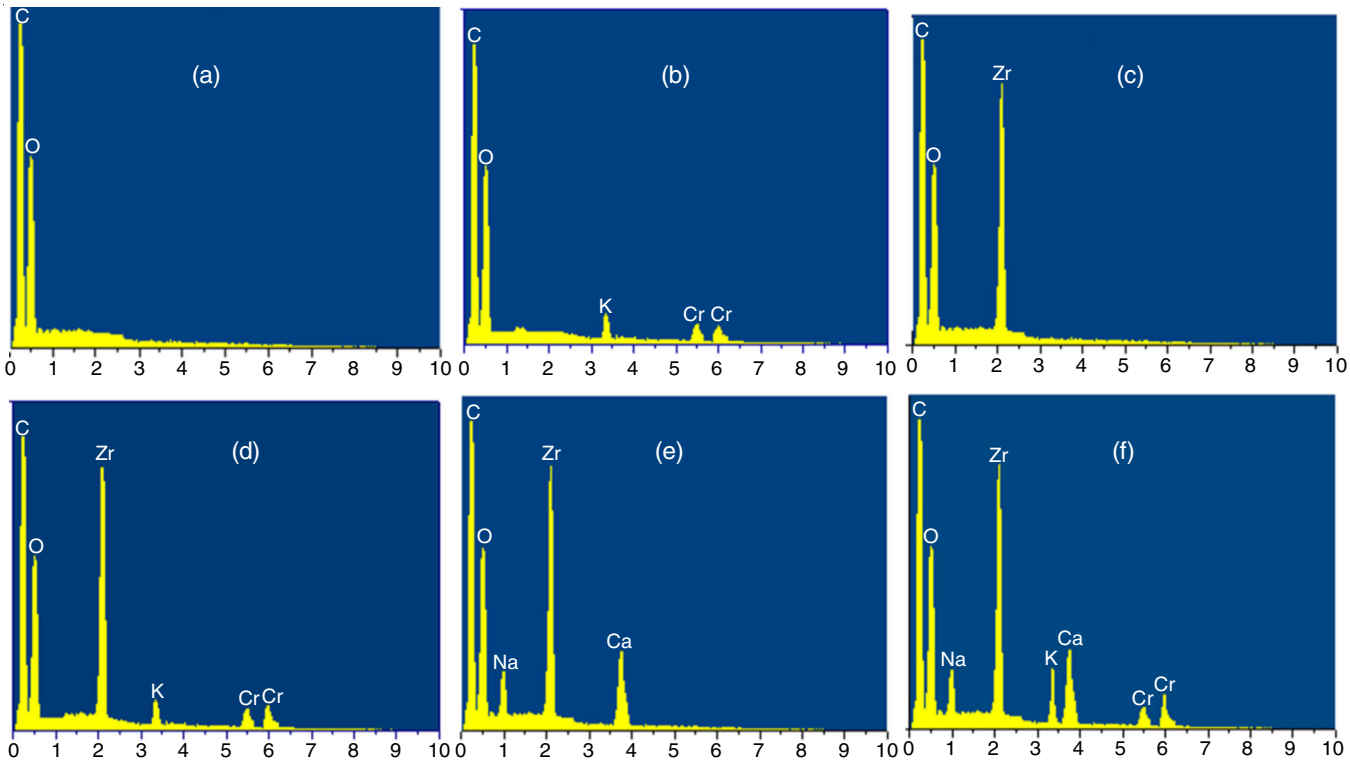

Fig. 4. EDX image of SACAR (before) (a); SACAR (after) (b); Zr-SACAR (before) (c); Zr-SACAR (after) (d); Zr-SACAR-Ca (before) (e) and Zr-SACAR-Ca after (f) Cr(VI) adsorption

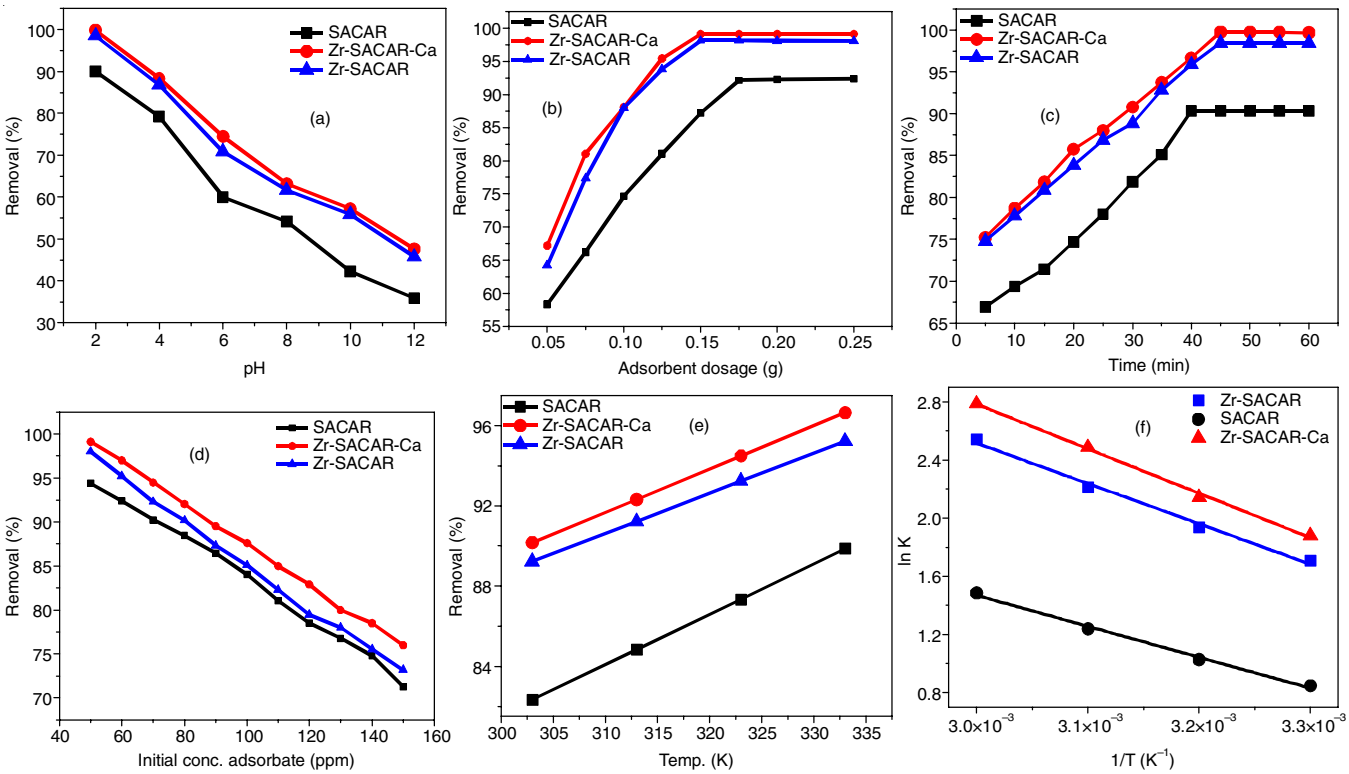

Fig. 5. Effect of pH (a), sorbent dosage (b), initial Cr(VI) concentration (c), contact time (d), temperature effect (e), and % removal of Cr(VI) (f)

with 0.175 g/100 mL for SACAR; 98.09% with 0.15 g/100 mL for Zr- SACAR and 99.14% with 0.15 g/100 mL for Zr-SACAR-Ca. With increase in the dosage of adsorbent, naturally the number of adsorption sites available increase and hence, more adsorption was observed initially. But when the adsorbent further increased, the extent of adsorption was not observed as that of the initial stages because the particles of the adsorbent get aggregated and thereby making less availability of sites

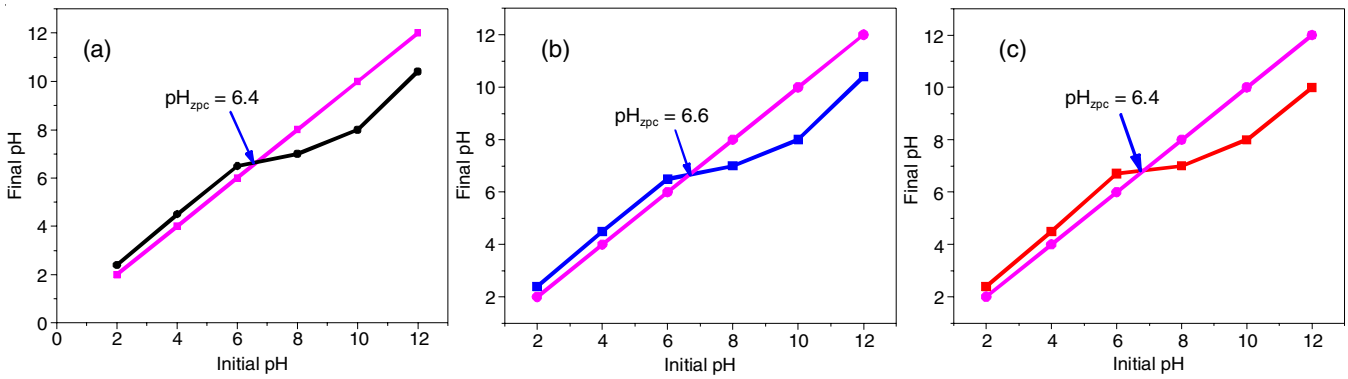

Fig. 6. Effect of pH$_{zpc}$ (a) SACAR (b) Zr-SACAR and (c) Zr-SACAR-Ca

for adsorption and further, the adsorbed chromium(VI) blocks or clogs the paths in the adsorbent matrix and thereby, prevents chromium(VI) to have proportional access to the internal pores of the adsorbents.

Effect of equilibration time: The influence of agitation time on the adsorption of Cr(VI) was studied by varying the time from 0 to 60 min while keeping the other extractions conditions at optimum levels namely: pH = 2: adsorbent conc.: 0.175 g/100 mL for SACAR, 0.15 g/100 mL Zr-SACAR and 0.15 g/100 mL for Zr-SACAR-Ca; initial concentration of Cr(VI) : 50 mg/L; rpm 300 and temperature 303 K. The plots of the percentage removal of Cr(VI) *vs.* contact time for adsorbents are shown in Fig. 5c.

The adsorption process was rapid initially but slow down with the progress of time and attained a steady state (with no further increase) after 40 min in the case of SACAR, 45 min with Zr-SACAR and Zr-SACAR-Ca. The high adsorption of Cr(VI) for a fixed amount of the adsorbent was due to the availability of more sites initially but with increase in the time, sites were progressively used up or blocked by the adsorbed Cr(VI) and hence, the rate of adsorption decreases. After certain minimum time, a steady state was resulted due to the complete occupation of the active site available in a fixed amount of the adsorbent. The maximum removal efficiencies of Cr(VI) were found to be 92.38% at 40 min for SACAR, 98.01% at 45 min for Zr-SACAR and 99.16% at 45 min for Zr-SACAR-Ca.

Initial Cr(VI) concentration-effect: By varying initial Cr(VI) concentration from 50 to 150 mg/L but maintaing other extraction conditions at optimum levels *viz*. pH 2; sorbent dosage 0.175 g/100 mL for SACAR, 0.15 g/100 mL for Zr-SACAR, 0.15 g/100 mL for Zr-SACAR-Ca; contact time 40 min for SACAR, 45 min for Zr-SACAR and Zr-SACAR-Ca at rpm 300 and temperature of 30 ± 1 ºC. (Fig. 5d). As the initial concentration of Cr(VI) increased from 50-150 mg/L, the % of extraction decreases from 92.2% to 70.8% for SACAR, 98.01% to 73.24% for Zr-SACAR and 100% to 76.5% for Zr-SACAR-Ca. As the concentration of Cr(VI) is increased, the demand for the active sites also increases. But as the adsorbent dosage is fixed, only limited active sites are available for adsorption. So, the availability of active sites per ion decreases with raise in Cr(VI) concentration and hence, adsorptivity decreases.

Thermodynamic investigations: The effect of temperature on adsorptivity of Cr(VI) was investigated at : 303, 313, 323 and 333 K for all the three adsorbents at optimum extraction conditions specified above (Fig. 5e and 5f). Enthalpy change (ΔH°), entropy change (ΔS°) and Gibbs free energy change (ΔG°) were evaluated as per conventional equations:

$$\Delta G = -RT \ln K_d \quad (3)$$

$$\ln k_d = \frac{\Delta S}{R} - \frac{\Delta H}{RT} \quad (4)$$

where ΔS is entropy change (J mol^{-1} K^{-1}), ΔH is enthalpy change (J mol^{-1}), ΔG is Gibbs free energy change (J mol^{-1}), R is the ideal gas constant (8.314 J mol^{-1} K^{-1}) and T is the absolute temperature (K). The ΔH and ΔS values were calculated using the van't Hoff plot and the plot of ln K$_d$ *vs.* 1/T is shown in Fig. 5f. The values of ΔH, ΔG and ΔS for the adsorption of Cr(VI) onto SACAR, Zr-SACAR and Zr-SACAR-Ca at various temperatures are given in Table-1, which inferred that as the temperature increases, ΔG values are more negative. This indicates the spontaneous of adsorption process with the raise in experimental temperature and so the adsorption process does not need require any external energy [28,29]. The more negative values of ΔG at elevated temperatures show the more favourability of adsorption process with increase in temperature [30]. It is interesting to note that the ΔG values are more negative in the order: SACAR< Zr-SACAR-Ca < Zr-SACAR-Ca. This indicates that the adsorption process is increasingly spontaneous and conducive in the same order. ΔH values for the three adsorbents are positive and they fall in the increasing order: SACAR < Zr-SACAR < Zr-SACAR-Ca. The positive values suggest the endothermic nature [31] and it indicates that the higher temperatures more favourable are the conditions to overcome the resistance for adsorption and thereby to accelerate the adsorption process.

Further using ΔH values, the adsorption nature can be assessed. The value of ΔH was 23.20 kJ/mol for Zr-SACAR and 30.5 kJ/mol for Zr-SACAR-Ca, which indicates that the adsorption process of Cr(VI) was chemical in nature [32]. But for SACAR, the value of ΔH was 17.70 kJ/mol indicating that the process was physical in nature [32]. The positive value of ΔS indicate that at the solid-liquid interface, the disorder is more and further, the value is increasing in the order: SACAR < Zr-SACAR < Zr-SACAR-Ca (Table-1). If the disorder is more, the randomness in the movement of the adsorbate at the surface is more and thereby the adsorbate penetrates deep into

TABLE-1A
THERMODYNAMICS PARAMETERS OF ADSORBENTS

Adsorbent	ΔH (kJ/mol)	ΔS (J/mol	ΔG (kJ/mol)				R^2
			303	313	323	333	
Zr-SACAR-Ca	30.5	99.64	-4.7	-5.7	-6.7	-7.7	0.997
Zr-SACAR	23.2	90.3	-4.3	-5.2	-6.1	-7.0	0.993
SACAR	17.7	65.3	-2.1	-2.74	-3.4	-4.15	0.991

TABLE-1B
ADSORPTION ISOTHERMS

Adsorbent	Parameters	Langmuir isotherm	Freundlich isotherm	Temkin isotherm	Dubinin-Radushkevich isotherm
Zr-SACAR-Ca	Slope	0.0125	0.305	13.02	-4.15E-06
	Intercept	0.0229	3.002	12.06	3.92
	R^2	0.970	0.990	0.96	0.727
	R_L/1/n/B/E	R_L = 0.26	1/n = 0.3056	B = 13.02	E = 0.35KJ/mol
Zr-SACAR	Slope	0.0129	0.238	11.41	-2.52E-06
	Intercept	0.053	3.390	27.28	4.03
	R^2	0.960	0.990	0.95	0.49
	R_L/1/n/B/E	R_L = 0.0759	1/n = 0.238	B =11.41	E = 0.445KJ/mol
SACAR	Slope	0.0125	0.183	9.7	-4.2E-07
	Intercept	0.023	3.714	41.51	4.09
	R^2	0.970	0.990	0.94	0.54
	R_L/1/n/B/E	R_L = 0.0355	1/n = 0.183	B = 9.7	E = 1.12 KJ/mol

TABLE-1C
KINETICS OF ADSORPTION

Adsorbents	Parameter	Pseudo-first order	Pseudo-second order	Elovoch	Bangham's pore diffusion
SACAR	Slope	-0.0274	0.05825	2.433155	0.14135
	Intercept	0.719	0.24637	5.54575	-1.53935
	R^2	0.955	0.99639	0.96616	0.95419
Zr-SACAR	Slope	-0.0194	0.05644	2.42812	0.14664
	Intercept	0.745	0.22798	6.4801	-1.56454
	R^2	0.958	0.99667	0.98797	0.95425
Zr-SACAR-Ca	Slope	-0.0151	0.08207	2.313395	0.16987
	Intercept	0.7640	0.35352	7.45182	-1.8845
	R^2	0.9750	0.99870	0.981353	0.973

the matrix of adsorbent and hence, adsorption is expected to increase in the same order [33].

Adsorption isotherms: The Freundlich (eqn. 5) [34], Langmuir (eqn. 6) [35], Temkin (eqn. 7) [36] and Dubinin and Radushkevich (eqn. 8) [37] isothermal models were employed to understand the adsorption mechanisms as described in the literature. The pertaining equations used are:

$$\ln q_e = \ln K_f + \frac{1}{n}\ln C_e \quad (5)$$

$$\frac{C_e}{q_e} = \frac{1}{K_L q_{max}} + \frac{1}{q_{max}} C_e \quad (6)$$

$$q_e = B \ln K_T + B \ln C_e \quad (7)$$

$$\ln q_e = -\beta\varepsilon + \ln q_m \quad (8)$$

It can be inferred from correlation coefficient (R^2) that Freundlich adsorption model has higher correlation coefficient: R^2 = 0.99 for all the three adsorbents: SACAR, Zr-SACAR and Zr-SACAR-Ca (Table-1) and so, it describes well the adsorption process. It indicates the heterogeneous surface of adsorbents as well as multi-layered adsorption. However, Langmuir and Temkin isotherm models are also equally valuable from the view point of correlation coefficients as R^2 values differ only in second decimals.

From the Freundlich plots (figures not shown), the values of 1/n were in the range $0.1 < 1/n < 1$ and further, they decrease in the order: SACAR > Zr-SACAR > Zr-SACAR-Ca. This reflects heterogeneous and multi-layer adsorption at the surface of adsorbents and it is probability decreases in the same order.

From the Langmuir isotherms (figures not shown), R_L values were calculated by using $R_L = 1 (1 + a_L C_0)$. The R_L values are 0.26 for SACAR, 0.0759 for Zr-SACAR and 0.0355 for Zr-SACAR-Ca. The extraction process is unfavourable if $R_L > 1$, linear if $R_L = 1$, favourable if: $0 < R_L < 1$ and irreversible if: $R_L = 0$. As R_L values for all the adsorbents are less than 1, the adsorption process is favourable. However, it is interesting to note that the values of Zr-SACAR and Zr-SACAR-Ca are tending towards zero, indicating more irreversibility of adsorption and maximum in the case Zr-SACAR-Ca. In other words, the physical nature of adsorption deceases while chemical nature of adsorption increases and more in Zr-SACAR-Ca.

Further, the adsorption process is modeled with the linear form of Temkin and Dubinin-Radushkevich equations. High values of regression coefficient of SACAR, Zr-SACAR and Zr-SACAR-Ca (Table-1) suggested a uniform distribution of binding energies over the number of exchangeable sites on the surface of the adsorbents

Kinetics of adsorption: The adsorption kinetics were evaluated by adopting various conventional models like pseudo-

first order (eqn. 9) [38], pseudo-second order (eqn. 10) [39], Bangham's pore diffusion model (eqn. 11) [40] and Elovich equation (eqn. 12) [41] as described in the literature. The concerned equations employed are:

$$\log(q_e - q_t) = \log q_e - \frac{k_1 t}{2.303} \quad (9)$$

$$\frac{t}{q_t} = \frac{1}{k_2 q_e^2} - \left(\frac{1}{q_e}\right) t \quad (10)$$

$$q_t = \frac{1}{\beta}\ln(\alpha\beta) + \frac{1}{\beta}\ln t \quad (11)$$

$$\log\left[\log\left(\frac{C_i}{C_i - q_t m}\right)\right] = \log\frac{k_1}{2.303V} + \alpha \log t \quad (12)$$

The R^2 values (Table-1) for the three sorbents fall in the order: Bangham's pore diffusion model < pseudo-first order model < Elovich model < pseudo-second-order. This indicates that the pseudo-second-order kinetics model describes well the adsorption process.

Interfering ions: The interference caused by two-fold excess of co-ions that naturally exists in water were investigated under the same optimum extraction conditions using SACAR, Zr-SACAR and Zr-SACAR-Ca as adsorbents. It may be noted that many of the cations as well as anions marginally affected the % of Cr(VI) extraction. SO_4^{2-} (84 %), PO_4^{3-} (88 %) and Zn^{2+} (86 %) have interfered to some extent (Fig. 7a-b).

Reusability of adsorbents: The resusability of all the three adsorbents *viz*. SACAR, Zr-SACAR and Zr-SACAR-Ca was investigated by treating the adsorbents with solutions of salts, bases and acids at various concentrations. It was observed that 0.01 N NaOH solution was effective in extracting Cr(VI) from the matrix of the adsorbent and thereby generating the adsorbent for re-use after washing with water and drying at 105 ºC. The number of cycles of regeneration of each adsorbent and their % removal are plotted in Fig. 7c. For all the three adsorbents, up to the six cycles of regeneration, the loss of adsorption capacity is marginal. So, by repetitively adopting the same regenerated adsorbent, complete removal of Cr(VI) may be achieved.

Applications

Characterization of levels of Cr in tannery effluent in Ethiopia: Wastewaters from the Ethiopia Tannery Company is discharged into Leyole and Worka rivers located near Kombolcha city, Ethiopia. The river water is used for irrigation and fishing purposes by the rural communities living in the vicinity of the said rivers and thereby, the people are exposed to chromium toxicity. In this work, the developed SACAR, Zr-SACAR &Zr-SACAR-Ca adsorbents were applied to remove Cr(VI) from water collected from Leyole and Worka rivers. The results are presented in Table-2, which inferred significant amounts of chromium is removed.

Comparative study: The procedures developed in this work with respect to the SACAR, Zr-SACAR and Zr-SACAR-Cafor the removal of Cr(VI) are compared with the previous works and summarized in Table-3. It can be inferred that the adsorption capacities of SACAR (92.2 mg/g), Zr-SACAR (109.83 mg/g) and Zr-SACAR-Ca (119.34 mg/g) are more than reported works in the literature.

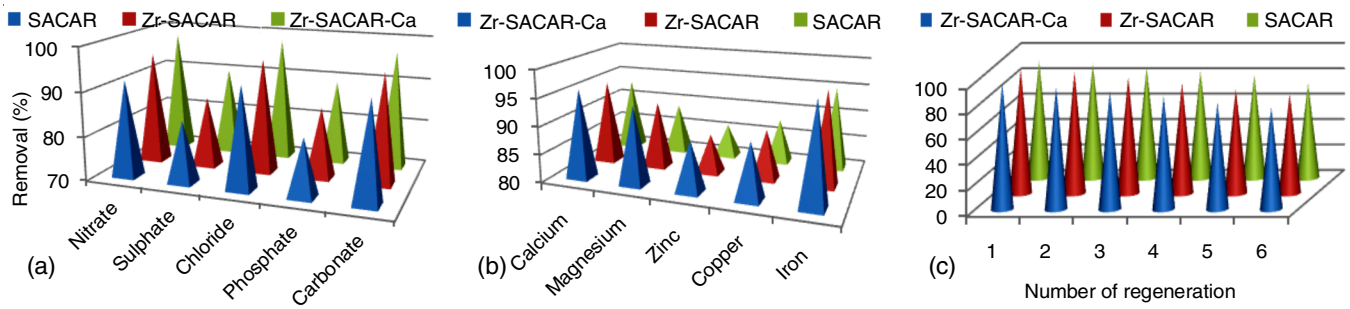

Fig. 7. Interference of Co-anions (a), Co-cations on the % removal of Cr (b) No. of regenerations *vs.* % removal (c)

TABLE-2
APPLICATIONS: TREATMENT OF Cr-POLLUTED WATER SAMPLES COLLECTED FROM THE RIVERS AROUND KOMBOLCHA CITY IN ETHIOPIA WITH THE ADSORBENTS DEVELOPED

Sample	Initial concentration of Cr(VI) in the collected samples [C_i (mg/L)]	SACAR		Zr-SACAR		Zr-SACAR-Ca	
		C_e (mg/L)	Extraction (%)	C_e (mg/L)	Extraction (%)	C_e (mg/L)	Extraction (%)
Samples collected in Leyole river							
1	3.5	0.2622	92.51	0	100	0	100
2	2.6	0.0983	96.22	0	100	0	100
3	4.4	0.4114	90.65	0.095	97.84	0	100
Samples collected in Worka river							
1	1.6	0	100	0	100	0	100
2	1.0	0	100	0	100	0	100
3	2.2	0.0559	97.46	0	100	0	100

TABLE-3
COMPARISON OF CHROMIUM UPTAKE CAPACITY WITH OTHER ADSORBENTS FROM LITERATURE

Adsorbent	Optimum pH	Initial concentration of Cr(VI) ions (mg/L)	Cr uptake capacity (mg/g)	Ref.
Magnetic MWCNTs	3.0	50	11.4	[42]
Carbon nano-tubes	4.0	50	9	[43]
RM modified by lanthanum	7.0	100	17.35	[44]
Magnetite nanoparticles	2.5	100	19.2	[45]
Humus supported nZVI	3.0	150	40.4	[46]
Biochar supported nano-ZnO	5.5	150	43.48	[47]
Chitosan-*g*-poly(butyl acrylate)/Si-gel	7.0	100	55.71	[48]
nZVI @ Fe_3O_4/Graphene	3.0	100	101	[49]
(nZVI)/Fe_3O_4 nanocomposite	8.0	50	29.43	[50]
SiO_2functionalized with sulphonic acid	3.0	150	72.8	[51]
SACAR	2.0	150	92.2	Present work
Zr-SACAR	2.0	150	109.83	Present work
Zr-SACAR-Ca	2.0	150	119.34	Present work

Conclusion

A good structured activated carbon was synthesized by digesting stems of *Annona reticulate* (SACAR) with conc. H_2SO_4 and utilized for the adsorptivity of toxic Cr(VI) ions. Nanoparticles of ZrO_2 of size 10-11 nm were successfully synthesized by adopting new green methods. Extract of sapindus plant seeds was found to be an effective capping/stabilizing agent in controlling the size of the particles. Three adsorbents were prepared with activated carbon and $nZrO_2$: (i) activated carbon (SACAR); (ii) composite of activated carbon + $nZrO_2$ (Zr-SACAR); and (iii) Zr-SACAR immobilized in Ca-alginate beads (Zr-SACAR-Ca). The efficiencies of these three adsorbents were investigated for their maximum adsorptivities for Cr(VI) ions by varying various extraction conditions. The kinetics of adsorption is well defined by the pseudo-second-order model. Thermodynamic parameters revealed that the nature of adsorption is endothermic and spontaneous. The adsorbents were reused until six cycles with marginal decrease adsorptivities. The adsorbents developed were also effectively applied for the removal of chromium(IV) ions from the water rivers samples collected from Ethiopia.

CONFLICT OF INTEREST

The authors declare that there is no conflict of interests regarding the publication of this article.

REFERENCES

1. H. Oliveira, *J. Botany*, **2012**, 375843 (2012); https://doi.org/10.1155/2012/375843
2. A. Zhitkovich, *Chem. Res. Toxicol.*, **24**, 1617 (2011); https://doi.org/10.1021/tx200251t
3. E. Parameswari, A. Lakshmanan and T. Thilagavathi, *J. Basic Appl. Sci.*, **3**, 1363 (2009).
4. M. Nur-E-Alam, M.A. Sayid Mia, F. Ahmad and M.M. Rahman, *Appl. Water Sci.*, **10**, 205 (2020); https://doi.org/10.1007/s13201-020-01286-0
5. A. Esmaeili, A. Mesdaghinia and R. Vazirineja, *Am. J. Appl. Sci*., **2**, 1471 (2009).
6. S.S. Chen, C.Y. Cheng, C.W. Li, P.H. Chai and Y.-M. Chang, *J. Hazard. Mater.*, **142**, 362 (2007); https://doi.org/10.1016/j.jhazmat.2006.08.029
7. S.K. Verma, V. Khandegar and A.K. Saroha, *J. Hazard. Toxic Radioact. Waste*, **17**, 146 (2013); https://doi.org/10.1061/(ASCE)HZ.2153-5515.0000170
8. S.A. Cavaco, S. Fernandes, M.M. Quina and L.M. Ferreira, *J. Hazard. Mater.*, **144**, 634 (2007); https://doi.org/10.1016/j.jhazmat.2007.01.087
9. G.V. Krishna Mohan, A. Naga Babu, K. Kalpana and K. Ravindhranath, *Int. J. Environ. Sci. Technol.*, **16**, 101 (2019); https://doi.org/10.1007/s13762-017-1593-7
10. S. Ravulapalli and R. Kunta, *Water Sci. Technol.*, **78**, 1377 (2018); https://doi.org/10.2166/wst.2018.413
11. M.T. Ahmed, S. Taha, T. Chaabane, D. Akretche, R. Maachi and G. Dorange, *Desalination*, **200**, 419 (2006); https://doi.org/10.1016/j.desal.2006.03.354
12. P.K. Meghana, K.V. Pravalika, P.J. Sriram and K. Ravindhranath, *Asian J. Chem.*, **31**, 1327 (2019); https://doi.org/10.14233/ajchem.2019.21760
13. Y.H. Rao and K. Ravindhranath, *Rasayan J. Chem.*, **10**, 1104 (2017); https://doi.org/10.7324/RJC.2017.1041829
14. A.N. Babu and G.K. Mohan, *Int. J. ChemTech Res.*, **9**, 506 (2016).
15. S. Ravulapalli and R. Kunta, *J. Fluorine Chem.*, **193**, 58 (2017); https://doi.org/10.1016/j.jfluchem.2016.11.013
16. S. Ravulapalli and K. Ravindhranath, *J. Taiwan Inst. Chem. Eng.*, **101**, 50 (2019); https://doi.org/10.1016/j.jtice.2019.04.034
17. A. Naga Babu, D.S. Reddy, G.S. Kumar, K. Ravindhranath and G.V. Krishna Mohan, *J. Environ. Manage.*, **218**, 602 (2018); https://doi.org/10.1016/j.jenvman.2018.04.091
18. S. Ravulapalli and K. Ravindhranath, *J. Anal. Methods Chem.*, **2017**, Article ID 3610878 (2017); https://doi.org/10.1155/2017/3610878
19. W.K. Biftu, K. Ravindhranath and M. Ramamoorty, *Nanotechnol. Environ. Eng.*, **5**, 12 (2020); https://doi.org/10.1007/s41204-020-00076-y
20. K. Ravindhranath and M. Ramamoorty, *Orient. J. Chem.*, **33**, 1603 (2017); https://doi.org/10.13005/ojc/330403
21. K. Ravindhranath and R. Mylavarapu, *Res. J. Chem. Environ.*, **21**, 42 (2017).
22. N. Savage and M.S. Diallo, *J. Nanopart. Res.*, **7**, 331 (2005); https://doi.org/10.1007/s11051-005-7523-5
23. B. Qiu, H. Gu, X. Yan, J. Guo, Y. Wang, D. Sun, Q. Wang, M. Khan, X. Zhang, B.L. Weeks, D.P. Young, Z. Guo and S. Wei, *J. Mater. Chem. A Mater. Energy Sustain.*, **2**, 17454 (2014); https://doi.org/10.1039/C4TA04040F
24. I. Ali, *Chem. Rev.*, **112**, 5073 (2012); https://doi.org/10.1021/cr300133d
25. A.I. Vogel, Text-Book of Quantitative Inorganic Analysis including Elementary Instrumental Analysis, Longmans, Green and Co., Ltd., London (1961).
26. W.K. Biftu and K. Ravindhranath, *Water Sci. Technol.*, **81**, 2617 (2020); https://doi.org/10.2166/wst.2020.318
27. R.K. Trivedy, Environmental Publications, Karad, India, edn 2 (1995).
28. C. Fan and Y. Zhang, *J. Geochem. Explor.*, **188**, 95 (2018); https://doi.org/10.1016/j.gexplo.2018.01.020

29. K.C. Bedin, A.C. Martins, A.L. Cazetta, O. Pezoti and V.C. Almeida, *Chem. Eng. J.*, **286**, 476 (2016); https://doi.org/10.1016/j.cej.2015.10.099
30. C.E. Rodrigues, K.K. Aracava and F.N. Abreu, *Int. J. Food Sci. Technol.*, **45**, 2407 (2010); https://doi.org/10.1111/j.1365-2621.2010.02417.x
31. W.S. Wan Ngah and M.A.K.M. Hanafiah, *Biochem. Eng. J.*, **39**, 521 (2008); https://doi.org/10.1016/j.bej.2007.11.006
32. C. Sun, C. Li, C. Wang, R. Qu, Y. Niu and H. Geng, *Chem. Eng. J.*, **200-202**, 291 (2012); https://doi.org/10.1016/j.cej.2012.06.007
33. L. Borah, M. Goswami and P. Phukan, *J. Environ. Chem. Eng.*, **3**, 1018 (2015); https://doi.org/10.1016/j.jece.2015.02.013
34. H.M.F. Freundlich, *J. Phys. Chem.*, **57**, 385 (1906).
35. I. Langmuir, *J. Am. Chem. Soc.*, **40**, 1361 (1918); https://doi.org/10.1021/ja02242a004
36. M. J. Temkin and V.Pyzhev, *Acta Physicochimica URSS*, **12**, 217 (1940).
37. M.M. Dubinin, *Dokl. Akad. Nauk SSSR*, **55**, 327 (1947).
38. J.F. Corbett, *J. Chem. Educ.*, **49**, 663 (1972); https://doi.org/10.1021/ed049p663
39. Y.S. Ho and G. McKay, *Process Biochem.*, **34**, 451 (1999); https://doi.org/10.1016/S0032-9592(98)00112-5
40. Y.S. Ho, J.C.Y. Ng and G. McKay, *Sep. Purif. Methods*, **29**, 189 (2000); https://doi.org/10.1081/SPM-100100009
41. S.K. Lagergren, *Sven. Vetenskapsakad. Handingarl*, **24**, 1 (1898).
42. Z.N. Huang, X.L. Wang and D.S. Yang, *Water Sci. Eng.*, **8**, 226 (2015); https://doi.org/10.1016/j.wse.2015.01.009
43. M.A. Atieh, *Procedia Environ. Sci.*, **4**, 281 (2011); https://doi.org/10.1016/j.proenv.2011.03.033
44. Y.W. Cui, J. Li, Z.F. Du and Y.Z. Peng, *PLoS One*, **11**, (2016); https://doi.org/10.1371/journal.pone.0161780
45. P. Yuan, D. Liu, M. Fan, D. Yang, R. Zhu, F. Ge, J.X. Zhu and H. He, *J. Hazard. Mater.*, **173**, 614 (2010); https://doi.org/10.1016/j.jhazmat.2009.08.129
46. R. Fu, X. Zhang, Z. Xu, X. Guo, D. Bi and W. Zhang, *Separ. Purif. Tech.*, **174**, 362 (2017); https://doi.org/10.1016/j.seppur.2016.10.058
47. J. Yu, C. Jiang, Q. Guan, P. Ning, J. Gu, Q. Chen, J. Zhang and R. Miao, *Chemosphere*, **195**, 632 (2018); https://doi.org/10.1016/j.chemosphere.2017.12.128
48. R. Nithya, T. Gomathi, P.N. Sudha, J. Venkatesan, S. Anil and S.K. Kim, *Int. J. Biol. Macromol.*, **87**, 545 (2016); https://doi.org/10.1016/j.ijbiomac.2016.02.076
49. X. Lv, X. Xue, G. Jiang, D. Wu, T. Sheng, H. Zhou and X. Xu, *J. Colloid Interface Sci.*, **417**, 51 (2014); https://doi.org/10.1016/j.jcis.2013.11.044
50. X. Lv, J. Xu, G. Jiang, J. Tang and X. Xu, *J. Colloid Interface Sci.*, **369**, 460 (2012); https://doi.org/10.1016/j.jcis.2011.11.049
51. S.E. Gomez-Gonzalez, G.G. Carbajal-Arizaga, R. Manriquez-Gonzalez, W. De la Cruz-Hernandez and S. Gomez-Salazar, *Mater. Res. Bull.*, **59**, 394 (2014); https://doi.org/10.1016/j.materresbull.2014.07.035